THE ASTROPHYSICAL JOURNAL, 376:599–607, 1991 August 1

THE SPECTRUM OF NGC 7027 FROM 3080 TO 2630 WAVENUMBERS (3.25–3.80 MICRONS): DETECTION OF NEW ATOMIC AND MOLECULAR HYDROGEN LINES AND NEW CONSTRAINTS ON THE CHEMICAL SIDEGROUPS ON POLYCYCLIC AROMATIC HYDROCARBONS

SCOTT A. SANDFORD[1]
NASA/Ames Research Center, MS 245-6, Moffett Field, CA 94035
Received 1990 December 21; accepted 1991 January 30

ABSTRACT

An infrared spectrum of NGC 7027, with a resolving power of 890–930 over the 2790–2690 cm^{-1} (3.58–3.72 μm) range, is presented which shows several emission lines due to atomic and molecular hydrogen. Three of the lines fall near 2773, 2743, and 2710 cm^{-1} (3.606, 3.645, and 3.690 μm) and are identified with the (20 → 6), (19 → 6), and (18 → 6) Humphreys series transitions of atomic hydrogen, respectively. The strengths of these lines are consistent with those expected from the observed intensity of the Pfund-γ (8 → 5) line in this object. The fourth line falls near 2760 cm^{-1} (3.623 μm) and is tentatively identified with the (0 → 0) $S(15)$ transition of molecular hydrogen. It is not presently clear whether the strength of the newly observed (0 → 0) $S(15)$ H_2 line relative to the previously detected H_2 lines in this object is consistent with shock excitation or fluorescence from clumpy photodissociation regions.

It is difficult to reconcile the relative strengths of the 3040, 2940, 2890, and 2850 cm^{-1} (3.29, 3.40, 3.46, and 3.51 μm) emission features in the spectrum of NGC 7027 with an origin in aliphatic sidegroups on polycyclic aromatic hydrocarbons (PAHs). The inconsistencies in the sidegroup model are minimized (but not eliminated) if the sidegroups are assumed to consist predominantly of methyl ($-CH_3$) groups. The absence of an emission feature centered near 2740 cm^{-1} (3.65 μm), which is characteristic of methyl groups attached to aromatics, places a severe upper limit on the number of methyl sidegroups that can be present in this object. If methyl groups are present at all, this upper limit implies that the PAH population in NGC 7027 must contain *at least* 400 peripheral aromatic C–H bonds for every peripheral methyl group. This $-CH_3$ abundance is a factor of 2–12 times too low to explain the strengths of the 2940, 2890, and 2850 cm^{-1} (3.40, 3.46, and 3.51 μm) features in the context of aliphatic sidegroups. Together these inconsistencies strongly indicate that the 2940, 2890, and 2850 cm^{-1} (3.40, 3.46, and 3.51 μm) interstellar emission features are *not* predominantly due to aliphatic sidegroups on PAHs.

Subject headings: infrared: spectra — interstellar: grains — line identifications — nebulae: individual (NGC 7027) — nebulae: planetary

1. INTRODUCTION

NGC 7027 is the brightest planetary nebula in the sky in the infrared. As a result, it is often used as a "test object," both for studies involving new techniques or instrumentation and in searches for new or predicted features that are expected to be weak. The spectroscopic attention that has been paid to this object in the infrared has resulted in the detection of a rich variety of atomic lines (e.g., Merrill, Soifer, & Russell 1975; Treffers et al. 1976; Bregman et al. 1983). A number of spectral features associated with molecular emission have also been detected, including lines due to H_2 (e.g., Treffers et al. 1976; Smith, Larson, & Fink 1981), CO (Masson et al. 1985), and the family of infrared emission features generally associated with polycyclic aromatic hydrocarbons (PAHs) and related aromatic materials (e.g., Russell, Soifer, & Willner 1977b; Russell, Soifer, & Merrill 1977a; Geballe et al. 1985; Witteborn et al. 1989).

The spectra presented here show contributions from both atomic and molecular hydrogen and from PAHs. The atomic and molecular hydrogen lines will be discussed only briefly, as it is the primary purpose of this paper to address several issues related to the PAH features. One of the characteristics of objects that produce the family of emission features associated with aromatic materials is the presence of several bands in the 3300–2800 cm^{-1} (3.0–3.6 μm) region. This region is dominated by a band near 3040 cm^{-1} (3.29 μm) (e.g., Merrill et al. 1975; Russell et al. 1977a, b; Geballe et al. 1985; Nagata et al. 1988) that is generally attributed to the fundamental C–H stretching vibrations of the H atoms on the outer rings of the PAHs (Duley & Williams 1981; Allamandola, Tielens, & Barker 1985, 1989). In most objects, this feature is attended by several weaker features near 2940, 2890, 2850, and 2810 cm^{-1} (3.40, 3.46, 3.51, and 3.56 μm) that lie on top of a broad emission plateau that extends from about 2990 to 2780 cm^{-1} (3.35–3.60 μm). These features show a tendency to decrease in strength with increasing wavelength and have been clearly detected in the spectrum of NGC 7027 (Geballe 1983; Nagata et al. 1988). The source of these weaker bands is presently a point of controversy and two distinctly different suggestions have been advanced to explain them, namely (1) anharmonicity of the aromatic C–H stretching vibration (Barker, Allamandola, & Tielens 1987; Allamandola et al. 1989), and (2) C–H stretching vibrations within sidegroups on the PAHs (Duley & Williams

[1] Visiting Astronomer, Infrared Telescope Facility, which is operated by the University of Hawaii under contract with the National Aeronautics and Space Administration.

1981; Jourdain de Muizon, et al. 1986; Jourdain de Muizon, d'Hendecourt, & Geballe 1990; Nagata et al. 1988).

The first suggestion is based on the fact that the potential energy well associated with the C–H stretching vibration in simple aromatic molecules is substantially anharmonic (Swofford, Long, & Albrecht 1976; Reddy, Heller, & Berry 1982). Since there is generally sufficient energy in the average interstellar UV photon to populate several levels of the C–H stretching mode in interstellar PAHs, the spectra should contain emission contributions from transitions such as $v = 3 \rightarrow 2$ and $v = 2 \rightarrow 1$ in addition to the fundamental $v = 1 \rightarrow 0$ transition. Because of the anharmonicity, however, the emissions from these higher energy levels are expected to fall at slightly lower frequencies than the 3040 cm^{-1} (3.29 μm) $v = 1 \rightarrow 0$ transition. Under this scheme the 3040, 2940, and 2850 cm^{-1} (3.29, 3.40, and 3.51 μm) bands are then assigned to the $v = 1 \rightarrow 0$, $v = 2 \rightarrow 1$, and $v = 3 \rightarrow 2$ transitions, respectively, of the C–H stretching vibration in an abundant PAH or PAHs (Barker et al. 1987). The features near 2890 and 2810 cm^{-1} (3.46 and 3.56 μm) may then originate from less abundant or less excited PAHs with slightly different anharmonicities, from overtones and combination bands of CC stretching vibrations, or from sidegroups.

An alternative explanation for the assignment of the lower frequency bands is that they are due to C–H stretching vibrations in methyl ($-CH_3$), methylene ($-CH_2-$), and perhaps aldehydic ($-CHO$) sidegroups on the PAHs (Duley & Williams 1981; Jourdain de Muizon et al. 1986, 1990). In this case, the weak features would be associated with specific functional groups replacing the peripheral H atoms on the PAHs. Since simple saturated aliphatic sidegroups on hydrogenated, neutral PAHs do not produce bands at the exact positions of the observed astronomical features, it has been suggested that the bands may be due to sidegroups on ionized, dehydrogenated, or electronically highly excited PAHs where the bands might be shifted (Jourdain de Muizon et al. 1986, 1990).

There is presently no consensus as to which of these suggestions is correct (indeed, some contribution by both might be required to explain *all* the observed bands), although evidence is building against sidegroups being responsible for most of the bands. In particular, the predictions of the sidegroup model are inconsistent with the observed spatial behavior of the features in the Orion Bar (Geballe et al. 1989). The importance of resolving the uncertainty of the source of these bands extends beyond their identification since the presence or absence of sidegroups on the PAHs will have profound effects on their chemical properties, spectral characteristics, and inferred histories (Allamandola et al. 1989).

This study was carried out in an attempt to better understand the source of these weak bands. The discussion of sidegroups on PAHs in NGC 7027 is divided into two main parts. In the first, limitations that can be placed on the presence of sidegroups by the observed relative strengths of the 3040, 2940, 2890, 2850, and 2810 cm^{-1} (3.29, 3.40, 3.46, 3.51, and 3.56 μm) features are discussed. The rationale followed is similar to that used for the 3040 and 2940 cm^{-1} (3.29 and 3.40 μm) bands by Geballe et al. (1989) for the Orion Bar and HD 44179. This is followed by a discussion of the results of a search for an emission band near 2740 cm^{-1} (3.65 μm) that would be expected to be present if methyl groups are present on the PAHs. The nondetection of a feature at this position provides an additional, tighter constraint on the abundance of sidegroups on the PAHs in this object.

2. OBSERVATIONS AND DATA REDUCTION

The observations were made using the 3 m NASA Infrared Telescope Facility (IRTF) on 1989 August 8 and 1990 July 27. Spectra were obtained using the LN_2-cooled, 32 InSb detector, Cooled-Grating Array Spectrometer (CGAS). The performance and configuration of this instrument is described in detail in Tokunaga, Smith, & Irwin (1987). At the time of operation, detectors 1, 2, 13, and 32 were not working reliably on the CGAS and the output from these detectors was not used. The 1989 August 8 low-resolution data were taken using grating A, which has 75 grooves mm^{-1} and provides a resolution of 0.018 μm per detector ($\lambda/\Delta\lambda = 180$–$210$ over the 3080–2630 cm^{-1} [3.25–3.80 μm] range). The 1990 July 27 high-resolution data were taken using grating B, which has 300 grooves mm^{-1} and a resolution of 0.004 μm per detector ($\lambda/\Delta\lambda = 890$–$930$ over the 2790–2690 cm^{-1} [3.58–3.72 μm] range). Both gratings were used in first order. Wavelength calibration was achieved in second order by comparison with the 5901 cm^{-1} (1.695 μm) line of an argon lamp. The detector spacing on the CGAS provides one detector per resolution element. The CGAS has a fixed aperture of 2".7 diameter.

Sky subtraction was accomplished through alternatively measuring NGC 7027 and nearby sky by nodding the telescope 30" EW. Correction for atmospheric absorption and flux calibration was accomplished by comparison with BS 8028 (ν Cygni) whose spectrum was measured through a similar air mass on the same night (usually within an hour) that NGC 7027 was observed. No further telluric extinction corrections were made to the data since the average air masses of NGC 7027 and BS 8028 differed by less than 0.03 air masses. BS 8028 has a spectral type of Al Vn, and the flux calibrations were made assuming a color temperature of 9120 K and an L magnitude of 3.86 (Tokunaga 1986). Fluxes are based on a 0.0 mag flux of 7.3×10^{-11} W m^{-2} μm^{-1} at L (3.45 μm). The resulting calculated fluxes are in reasonable agreement with published photometry values for this object.

3. DISCUSSION

The new high- and low-resolution spectra of NGC 7027 are presented in Figure 1. As expected, two of the most prominent features in the figure are the 3040 cm^{-1} (3.29 μm) and 2940 cm^{-1} (3.40 μm) emission bands associated with PAHs. Also apparent is a feature near 2675 cm^{-1} (3.74 μm) which, following Merrill et al. (1975), I identify with the Pfund-γ ($8 \rightarrow 5$) atomic hydrogen transition. The increasingly weaker PAH bands at 2890, 2850, and 2810 cm^{-1} (3.46, 3.51, and 3.56 μm) are not individually apparent due to the low resolution of the 3080–2630 cm^{-1} (3.25–3.80 μm) spectrum. Instead they are blended together with the underlying plateau as an extended "wing" to the red of the 2940 cm^{-1} (3.40 μm) feature (although the 2890 cm^{-1} [3.46 μm] feature is marginally apparent). The high-resolution spectrum in the 2790–2690 cm^{-1} (3.58–3.72 μm) range is replotted on an expanded scale in Figure 2 and contains four narrow emission lines. The spectrum in Figure 2 is interpreted in detail in the following three subsections of the paper.

3.1. *Hydrogen Lines*

3.1.1. *Atomic Hydrogen*

The three weakest lines in Figure 2 fall near 2773, 2743, and 2710 cm^{-1} (3.606, 3.645, and 3.690 μm). These are near the

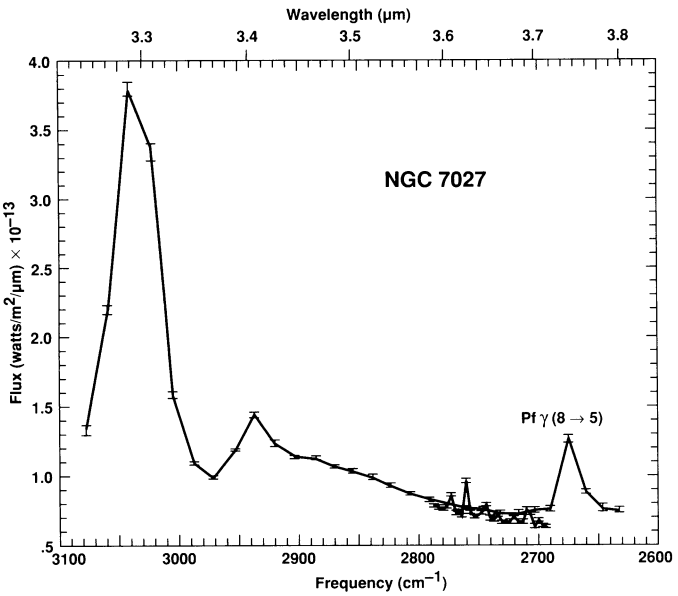

FIG. 1.—The low- and high-resolution spectra of NGC 7027. The low-resolution spectrum was taken on 1989 August 8 and has a resolution of 0.018 μm per detector ($\lambda/\Delta\lambda$ = 180–210 over the 3080–2630 cm^{-1} [3.25–3.80 μm] range shown). The high-resolution spectrum was taken 1990 July 27 and has a resolution of 0.004 μm per detector ($\lambda/\Delta\lambda$ = 890–930 over the 2790–2690 cm^{-1} [3.58–3.72 μm] range shown). The prominent 3040 cm^{-1} (3.29 μm) and 2940 cm^{-1} (3.40 μm) PAH bands and the 2675 cm^{-1} (3.74 μm) Pfund-γ (8 → 5) hydrogen line are all apparent in the low-resolution spectrum. Points without error bars have errors smaller than the points themselves.

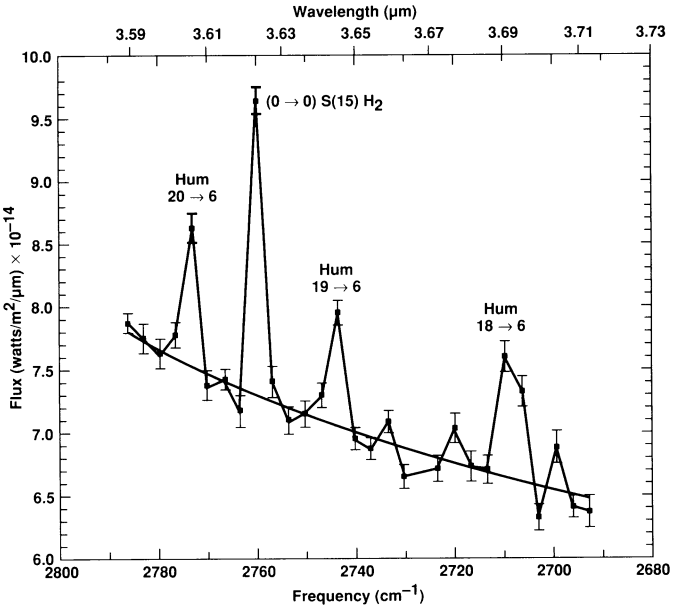

FIG. 2.—An expanded plot of the high-resolution spectrum shown in Fig. 1. The emission lines due to the Humphreys series (20 → 6), (19 → 6), and (18 → 6) hydrogen transitions are labeled, as is the line tentatively identified with the (0 → 0) S(15) molecular hydrogen transition. The baseline was derived by fitting a second-order polynomial to the data set after the atomic and molecular hydrogen lines were removed.

expected frequencies of the (20 → 6), (19 → 6), and (18 → 6) Humphreys series, atomic hydrogen transitions, respectively (Wiese, Smith, & Glennon 1966). Since the electron temperature and density in NGC 7027 have been determined, it is possible to use the Pfund-γ (8 → 5) line in Figure 1 to calculate the expected strength of the Humphreys series. For NGC 7027, Merrill et al. (1975) have reported values of $T_e = 2 \times 10^4$ K and $n_e = 1 \times 10^4$ cm^{-3}, while Treffers et al. (1976) report a slightly lower temperature of $T_e = 1.5 \times 10^4$ K. The expected strengths of the three Humphreys lines was determined using the table appropriate for $T_e = 1 \times 10^4$ K and $n_e = 1 \times 10^4$ cm^{-3} from Hummer & Storey (1987) and scaling to the observed strength of the Pfund-γ (8 → 5) line. The predicted and observed values are compared in Table 1. The predicted and observed line strengths agree within the uncertainties associated with the measured band intensities and the slight mismatch in electron temperature between NGC 7027 and the model calculations used. This strongly supports the identification of these three lines with atomic hydrogen. Finally, the identification of these bands with the hydrogen Humphreys series is in agreement with the identification of the (21 → 6), (22 → 6), (23 → 6), (24 → 6), (25 → 6), and possibly the (26 → 6), Humphreys transitions in a different, adjacent spectrum of NGC 7027 reported by Nagata et al. (1988). Thus, the 2773, 2743, and 2710 cm^{-1} (3.606, 3.645, and 3.690 μm) emission lines are identified as being due to the (20 → 6), (19 → 6), and (18 → 6) Humphreys series transitions of atomic hydrogen.

3.1.2. *Molecular Hydrogen*

The strongest emission line in the spectrum in Figure 2 falls near 2760 cm^{-1} (3.623 μm). This is in good agreement with the frequency of 2758.9 cm^{-1} (3.6246 μm) for the (0 → 0) S(15)

TABLE 1

OBSERVED AND EXPECTED STRENGTHS OF THE PFUND-γ (8 → 5) LINE AND THE (20 → 6), (19 → 6), AND (18 → 6) HUMPHREYS LINES

Emission Line	Observed Band Intensity (W m^{-2})[a]	Observed Ratio Pfund-γ (8 → 5) Line	Expected Ratio Pfund-γ (8 → 5)[b] Line
Pfund-γ (8 → 5)	1.2×10^{-15}[c]	1.0	1.0
Humphreys (18 → 6)	8.8×10^{-17}[d]	13.8	19.0
Humphreys (19 → 6)	5.0×10^{-17}[d]	24.0	22.5
Humphreys (20 → 6)	5.9×10^{-17}[d]	20.5	26.2

[a] Band intensities are estimated to be accurate to about 25%.
[b] From Table 6 of Hummer & Storey 1987.
[c] Measured from the low-resolution data presented in Fig. 1.
[d] Measured from the high-resolution data presented in Fig. 2.

transition of molecular H_2 (T. Geballe, private communication). Infrared lines due to molecular H_2 have already been identified in the spectrum of NGC 7027. The $(1 \rightarrow 0)$ $S(1)$ line at 4712.9 cm^{-1} (2.1218 μm) and the $(1 \rightarrow 0)$ $Q(1)$ and $(1 \rightarrow 0)$ $Q(3)$ lines at 4155.3 and 4125.9 cm^{-1} (2.4066 and 2.4237 μm), respectively, were first reported by Treffers et al. (1976). Smith et al. (1981) subsequently verified the presence of these three lines and detected additional $(1 \rightarrow 0)$ H_2 lines in the 6250–4000 cm^{-1} (1.6–2.5 μm) region. They reported that the H_2 line strengths suggested a model in which the emitting H_2 gas is confined to clumps heated in a shock front accompanied by an expanding H II region, i.e., the H_2 emission comes largely from the outer envelope of the planetary nebula.

It is not presently clear whether the identification of the 2760 cm^{-1} (3.623 μm) $(0 \rightarrow 0)$ $S(15)$ line in the spectrum of this object is consistent with a shock-induced emission model. The excitation temperature of the $(1 \rightarrow 0)$ $S(1)$ line is about 7000 K, while the excitation temperature of the $(0 \rightarrow 0)$ $S(15)$ line is over 21,000 K (Burton, Hollenbach, & Tielens 1990), a very high excitation for a shocked region. The $S(1)/S(15)$ intensity ratio for a jump shock with dissociational cooling is expected to be about 6–8 for the densities and shock velocities appropriate for NGC 7027 (M. Burton, private communication). The reported strength of the $(1 \rightarrow 0)$ $S(1)$ H_2 line in NGC 7027 is 2.8×10^{-15} W m^{-2} (Smith et al. 1981). This compares to a band intensity of 1.2×10^{-16} W m^{-2} for the $(0 \rightarrow 0)$ $S(15)$ H_2 line reported here. Scaling these intensities by a factor of 6.7 to account for aperture size differences (7″ versus 2.″7) leads to an observed $S(1)/S(15)$ intensity ratio of about 3.5, i.e., a factor of about 2 times lower than the value calculated from the jump shock model.

An alternative explanation involving fluorescence might be considered. It is interesting to note that both the [O I] and [C II] line emission (Ellis & Werner 1984) and strong FUV radiation field in NGC 7027 indicate that a photodissociation region is present. Fluorescence from this photodissociation region would be expected to contribute to the H_2 line emission as well. The $S(1)/S(15)$ intensity ratio from the photodissociation region appropriate for NGC 7027 is expected to be about 8–15 (M. Burton, private communication; Burton et al. 1989). This value is ~ 3 times larger than the observed value of 3.5.

Differential extinction due to intervening interstellar grains is not sufficiently large to account for the apparent excess brightness of the $S(15)$ line. Thus, to first appearance, the observed strength of the $(0 \rightarrow 0)$ $S(15)$ H_2 line is too strong to find an easy explanation in terms of either shocks *or* simple UV-excited fluorescence, although the former comes closest. This difficulty could well be due to the use of different apertures in the measurement of the different lines. If the H_2 emission is "clumpy" or is concentrated at the boundary of the planetary nebula, the observed intensity would be expected to be dependent on both aperture size and beam placement. Indeed, there is some evidence that the extinction toward NGC 7027 may be clumpy at infrared wavelengths (Seaton 1979). However, if the intensity of the $(0 \rightarrow 0)$ $S(15)$ H_2 line really is as large as the comparison made here suggests, then the intriguing possibility that an inverted level population may be present, with all the interesting physical phenomena that entails, is raised. Unfortunately, the intercomparison of data taken using different apertures is fraught with potential pitfalls. Clearly an investigation of the relative strengths of the $(0 \rightarrow 0)$ $S(15)$ and the various $(1 \rightarrow 0)$ lines using the same apertures and beam positions would be of interest.

3.2. *Constraints on the Abundance and Composition of the Chemical Sidegroups on the PAHs*

In this section, two independent means are used to place constraints on the abundance and composition of any chemical sidegroups that may exist on the PAHs in NGC 7027. The first expands on the rationale presented by Geballe et al. (1989) and places limits on the abundance of sidegroups using the observed relative strengths of the 3040 and 2940 cm^{-1} (3.29 and 3.40 μm) features. The second method involves the search for a weak emission band near 2740 cm^{-1} (3.65 μm) that would be expected to be present in the spectrum of NGC 7027 if methyl sidegroups are present on the PAHs. The detection or nondetection of a feature at this position provides a strong, additional, independent constraint on the abundance of PAH sidegroups in this object.

3.2.1. *Constraints from the Strengths of the* 3040–2850 cm^{-1} *Emission Features*

If we assume the 2940, 2890, and 2850 cm^{-1} (3.40, 3.46, and 3.51 μm) features are all due to saturated aliphatic sidegroups on PAHs, it is possible to use their observed strengths relative to the 3040 (3.29 μm) band to determine the relative numbers of H atoms in aromatic versus aliphatic sites along the line of sight. Since the energies required to excite the first energy level of these vibrational modes are very nearly identical, we would expect them to become essentially equally populated subsequent to the absorption of a UV photon. Thus, the relative number of C–H bonds of each type along the line of sight can be found by ratioing the observed integrated band areas and scaling by the ratio of the bands' intrinsic strengths (A values).

Aliphatic hydrocarbons generally produce bands near 2955 and 2870 cm^{-1} (3.385 and 3.485 μm) due to asymmetric and symmetric stretching vibrations in $-CH_3$ groups and near 2925 and 2860 cm^{-1} (3.420 and 3.495 μm) due to asymmetric and symmetric stretching vibrations in $-CH_2-$ groups, respectively (Bellamy 1960; Sandford et al. 1991). As noted earlier, these positions do not precisely match those of the bands seen in emission in NGC 7027. However, it has been suggested that these positions might be modified if the PAHs were ionized, dehydrogenated, or electronically highly excited (Jourdain de Muizon et al. 1986). For the sake of argument, I will therefore ignore the positional mismatches and proceed on the assumption that the C–H vibrations in aliphatics will be moved to the observed astronomical positions under the correct conditions.

3.2.2. *Limits from the* 2940 cm^{-1} (3.40 μm) *Emission Feature*

In this case, the 2940 cm^{-1} (3.40 μm) feature in NGC 7027 would most likely be associated with the asymmetric stretching vibrations that cause the 2955 cm^{-1} (3.385 μm) $-CH_3$ and 2925 cm^{-1} (3.420 μm) $-CH_2-$ bands in pure aliphatics. Unfortunately, the integrated band strengths for gas-phase PAHs with and without aliphatic sidegroups have not yet been accurately measured for the larger PAHs of direct astrophysical interest. If the relative strengths of the aliphatic and aromatic C–H stretching bands for benzene derivatives can be taken as representative of those for larger PAHs (a very reasonable assumption), then the absolute strength of the C–H stretching feature per C–H bond is 1–3.5 times weaker in aromatics than in the 2940 cm^{-1} (3.40 μm) saturated aliphatic band, with the average falling near a factor of 2 (Gribov & Smirnov 1962; Wexler 1967; Bishop & Cheung 1982, see also Sandford et al. 1991 for further discussion). I will assume for the purposes of this paper that, on a per C–H bond basis,

A(aliphatic) $\approx 2 \times A$(aromatic) for the vibrations that produce the 3040 and 2940 cm^{-1} (3.29 and 3.40 μm) features.

Geballe et al. (1985) report a value of ~ 0.06 for the ratio of the 2940 to 3040 cm^{-1} (3.40 to 3.29 μm) integrated band areas in the spectrum of NGC 7027, a value similar to that I measure off the spectrum of NGC 7027 in the paper by Nagata et al. (1988). Scaling this ratio by the relative aliphatic and aromatic A values then indicates that, in the context of the aliphatic sidegroup model, *there are approximately* 30 *aromatic* C–H *stretches for every aliphatic* C–H *stretch* along the line of sight. If all the aliphatic C–H bonds belong to methyl ($-CH_3$) groups, this corresponds to ~ 90 aromatic C–H bonds for every $-CH_3$ sidegroup present in NGC 7027.

The interstellar PAHs that dominate the infrared emission in this part of the spectrum are generally thought to consist predominantly of molecules having between about 20 and 40 carbon atoms (cf. Allamandola et al. 1989). It is also generally assumed that these molecules are largely in more condensed forms (for example, pyrene rather than anthracene; see Table 2), since these forms are expected to be more stable in the interstellar radiation environment (cf. Allamandola et al. 1989). Thus, the typical interstellar 20–40 C atom PAH will have 10–20 peripheral H atoms. If we assume that the "average" interstellar PAH carries 15 peripheral H atoms, then the preceding argument suggests that only about one in six of these molecules is carrying a methyl group. If we consider ethyl

TABLE 2

REPRESENTATIVE AROMATIC COMPOUNDS EXAMINED IN THIS STUDY

Structure	Name and Formula	Side Groups Examined[a]
	Benzene (C_6H_6)	methyl locations - 1,(1,4),(1,2,3),(1,2,4), (1,2,3,4),(1,2,3,5),(1,2,4,5),(1,2,3,4,5), (1,2,3,4,5,6) ethyl locations - 1,(1,2),(1,4),(1,3,5) + many combinations of methyl, ethyl, butyl, pentyl, decyl, and isopropyl groups
	Naphthalene ($C_{10}H_8$)	methyl locations - 1,2,(1,2),(1,3),(1,4),(1,5), (1,6),(1,7),(2,3), (2,6),(2,7),(1,10), (1,6,7), (2,3,6) ethyl locations - 1,2 + several combinations of methyl, butyl, pentyl, and isopropyl groups
	Anthracene ($C_{14}H_{10}$)	methyl locations - 2,9,(1,10),(2,10),(9,10), (1,3),(2,3),(2,6),(2,7), (2,9),(1,10), (2,3,6),(2,3,9),(1,6,10),(4,7,9), (2,3,9,10),(2,3,6,7),(2,3,6,7,9,10)
	Phenanthrene ($C_{14}H_{10}$)	methyl locations - 1,2,3,4,9,(2,3),(2,5), (2,7),(4,5),(9,10),(2,3,5),(2,3,9) ethyl locations - 9
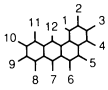	Benzo[a]anthracene ($C_{18}H_{12}$)	methyl locations - 1,2,3,4,5,6,7,8,9,10,11, 12,(7,12),(9,10)
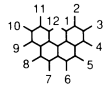	Benzo[c]phenanthrene ($C_{18}H_{12}$)	methyl locations - 1,2,3,4,5,6
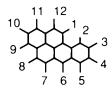	Benzo[a]pyrene ($C_{20}H_{12}$)	methyl locations - 12
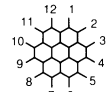	Coronene ($C_{24}H_{12}$)	methyl locations - 1 ethyl locations - 1
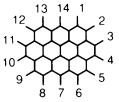	Ovalene ($C_{32}H_{14}$)	methyl locations - 7,(7,14)

[a] The numbers refer to the position(s) of the sidegroup on the PAH and correspond to the sites labeled on the associated molecular diagram. Single numbers refer to derivatives with one-sidegroup, two numbers in parentheses refer to derivatives with two-sidegroups, and so on. The formulas for the sidegroups mentioned are methyl [$-CH_3$], ethyl [$-CH_2CH_3$], propyl [$-(CH_2)_2CH_3$], butyl [$-CH_2)_3CH_3$], pentyl [$-(CH_2)_4CH_3$], decyl [$-(CH_2)_9CH_3$], and isopropyl $CH(CH_3)_2$].

($-CH_2-CH_3$) sidegroups instead of methyl sidegroups, the limit becomes even more restrictive. If all the sidegroups present in NGC 7027 were ethyl groups, there would have to be ~150 aromatic C–H stretches for every sidegroup present and the "average" PAH would have only about a one in 10 chance of carrying a sidegroup. Similar arguments can be made for propyl [$(-CH_2-)_2-CH_3$], butyl [$(-CH_2-)_3-CH_3$], and larger aliphatic sidegroups. Thus, it is clear from the relative strengths of the 3040 and 2940 cm^{-1} (3.29 and 3.40 μm) features that even if aliphatic sidegroups are responsible for the 2940 cm^{-1} (3.40 μm) emission feature, they are not abundant on interstellar PAHs. This conclusion is in general agreement with the conclusions drawn from observations of the 2940 cm^{-1} (3.40 μm) feature in the Orion Bar (Geballe et al. 1989).

3.2.3. *Limits from the* 2890 cm^{-1} (3.46 μm) *Emission Feature*

Similar arguments can be made for the 2890 cm^{-1} (3.46 μm) interstellar emission feature. In this case, the observed band would most likely be associated with the symmetric C–H stretching vibration within $-CH_3$ groups in pure aliphatics that produces a band near 2870 cm^{-1} (3.485 μm). This aliphatic band is weaker than those at 2955 and 2925 cm^{-1} (3.385 and 3.420 μm) and, on a per C–H bond basis, it is expected that A(aliphatic) $\approx 0.4 \times A$(aromatic) for this band (Sandford et al. 1991). Geballe et al. (1985) report a value of ~0.04 for the ratio of the 2890 to 3040 cm^{-1} (3.46 to 3.29 μm) integrated band areas in the spectrum of NGC 7027, also in good reasonable agreement with the value I measure from the spectrum of Nagata et al. (1988). Following the rationale presented for the 2940 cm^{-1} (3.40 μm) emission feature and in the context of the sidegroup model, this suggests a limit of *approximately* 10 *aromatic* C–H *stretches for every aliphatic* C–H *stretch* along the line of sight. This aliphatic abundance is a factor of 3 times larger than that obtained using the 2940 cm^{-1} (3.40 μm) feature. If all the aliphatic C–H bonds belong to methyl ($-CH_3$) groups, this corresponds to ~30 aromatic C–H stretches for every $-CH_3$ sidegroup present in NGC 7027.

3.2.4. *Limits from the* 2850 cm^{-1} (3.51 μm) *Emission Feature*

In this case, the observed interstellar emission feature would most likely be associated with the symmetric C–H stretching vibration within $-CH_2-$ groups in pure aliphatics that produces a band near 2860 cm^{-1} (3.495 μm). This aliphatic band is also weaker than the bands at 2955 and 2925 cm^{-1} (3.385 and 3.420 μm) and on a per C–H bond basis it is expected that A(aliphatic) $\approx 0.75 \times A$(aromatic) for this band (Sandford et al. 1991). Geballe et al. (1985) do not report a value for the ratio of the 2890–3040 cm^{-1} (3.46–3.29 μm) integrated band areas in the spectrum of NGC 7027, so I use the value of 0.013 which I measured from the spectrum of Nagata et al. (1988). Similar measurements from this spectrum of the other band ratios agreed with the values reported by Geballe et al. (1985) to within 20%. Scaling this ratio by the A values of the respective bands then yields a limit of *approximately* 60 *aromatic* C–H *stretches for every aliphatic* C–H *stretch* along the line of sight. This aliphatic abundance is a factor of 2 times smaller than that obtained using the 2940 cm^{-1} (3.40 μm) feature and 6 times smaller than that obtained using the 2890 cm^{-1} (3.46 μm) feature.

Since the 2860 cm^{-1} (3.495 μm) aliphatic C–H feature is associated with $-CH_2-$ groups, it cannot be due to methyl groups but must instead be associated with groups as large as, or larger than, ethyl ($-CH_2CH_3$) groups. Assuming the entire feature is produced by ethyl sidegroups, this corresponds to 300 aromatic C–H stretches for every ethyl group in NGC 7027.

3.2.5. *Incompatibilities between the Various Limits*

The aromatic-to-aliphatic C–H bond ratios derived above can be used to determine the relative numbers of aliphatic C–H bonds associated with each of the bands. The aliphatic-to-aromatic C–H bond ratios of 1/30, 1/10, and 1/60 derived from the 2940, 2890, and 2850 cm^{-1} (3.40, 3.46, and 3.51 μm) emission features, respectively, correspond to a relative ratio of 4 to 12 to 2 for the number of aliphatic bonds responsible for these three bands. These relative ratios are difficult to reconcile in terms of the presence of simple aliphatic sidegroups. The lowest aliphatic abundances are derived from the 2850 cm^{-1} (3.51 μm) feature (due entirely to $-CH_2-$ groups); the next highest aliphatic abundance is derived from the 2940 cm^{-1} (3.40 μm) feature (due to $-CH_2-$ *and* $-CH_3$ groups); and the highest abundance is derived from the 2890 cm^{-1} (3.46 μm) feature (due solely to $-CH_3$ groups). At first appearance this progression seems to suggest that sidegroups could be responsible for the features if $-CH_2-$ groups are considerably less abundant than $-CH_3$ groups.

However, a simple overabundance of $-CH_3$ groups raises serious inconsistencies. Taking into account the number of C–H bonds per $-CH_2-$ and $-CH_3$ group, the relative C–H bond abundance of 4 to 12 to 2 for the 2940 ($-CH_2-$ and $-CH_3$), 2890 ($-CH_3$ only) and 2850 ($-CH_2-$ only) cm^{-1} features corresponds to the relative abundances of approximately one $-CH_2-$ and one $-CH_3$ group (to produce the 2940 cm^{-1} feature) to 4 $-CH_3$ groups (to produce the 2890 cm^{-1} feature) to one $-CH_2-$ group (to produce the 2850 cm^{-1} feature). Thus, while the same $-CH_2-$ groups can be responsible for the appropriate contributions to the 2940 and 2850 cm^{-1} features, three additional $-H_3$ groups are *required* to produce the 2890 cm^{-1} band while simultaneously failing to show any contribution to the 2940 cm^{-1} band.

In conclusion, a careful comparison of the relative strengths of the 3040, 2940, 2890, and 2850 cm^{-1} (3.29, 3.40, 3.46, and 3.51 μm) interstellar emission features, interpreted using the sidegroup model, shows that *it is unlikely that the* 2940, 2890, *and* 2850 cm^{-1} (3.40, 3.46, *and* 3.51 μm) *interstellar emission features are predominantly due to aliphatic sidegroups on PAHs.* The inconsistencies created by the sidegroup model are minimized (but not eliminated) if the sidegroups are assumed to consist predominantly of methyl ($-CH_3$) groups. It is shown in the following section, however, that very tight constraints can be placed on the abundance of methyl groups on the PAHs in NGC 7027, and that these constraints lead to additional inconsistencies in the sidegroup model.

3.2.6. *Constraints from the Nondetection of the Methyl Deformation Overtone near* 2740 cm^{-1} (3.65 μm)

It was shown above that it is difficult to reconcile the relative strengths of the 2940, 2890, and 2850 cm^{-1} (3.40, 3.46, and 3.51 μm) interstellar emission features with an origin in aliphatic sidegroups on PAHs. The inconsistencies with the sidegroup model are minimized (but not removed) if the sidegroups consist predominantly of methyl ($-CH_3$) groups.

PAHs with methyl sidegroups typically produce a band in the 2750–2720 cm^{-1} (3.64–3.68 μm) region that has a FWHM of 20–40 cm^{-1} (see Fig. 3). This band was first noticed in the spectra of methylnaphthalene derivatives by Fox & Martin

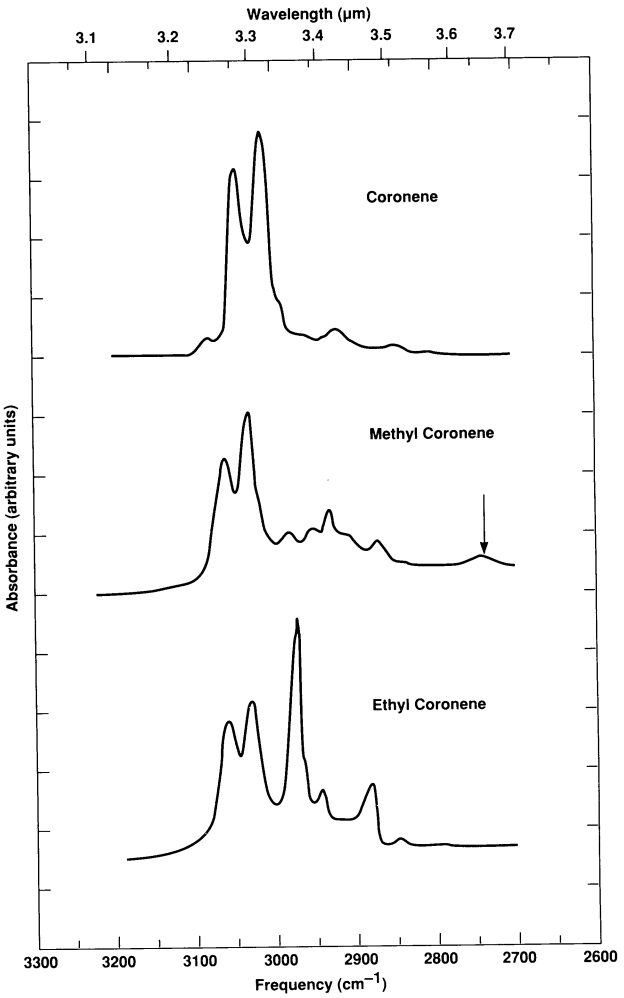

FIG. 3.—Spectra demonstrating that the 2740 cm^{-1} (3.65 μm) feature is present when a PAH has peripheral methyl groups, but that this band is absent when no sidegroups are present and considerably weaker or absent when ethyl groups are present. This behavior is observed for all the PAHs listed in Table 2. (The spectrum of coronene was adopted from Fig. 5 of Allamandola et al. 1989 and was taken by S. J. Cyvin and P. Klaeboe of the University of Trondheim, Norway [see also Cyvin et al. 1982]. The methyl and ethyl coronene spectra were taken from Fig. 5 of Jourdain de Muizon et al. 1990.)

(1939). Subsequently, Fuson & Josien (1956) noticed a similar band in the spectra of methylbenzanthracenes, and they suggested that "the most consistent 'identification tag' for the methylated aromatics is the weak but clearcut band at 2734 $\pm$ 5 cm^{-1}." In an attempt to verify that this statement can be generalized to all PAHs, I have made an extensive search of the laboratory infrared spectra of many different PAHs both with and without various (mostly aliphatic) sidegroups (Table 2). Almost without exception, PAHs free of sidegroups show no features in the 2800–2700 cm^{-1} (3.57–3.70 μm) region, while those with attached methyl groups do. The identification of this feature with the methyl groups is supported by the fact that the feature generally increases in strength as the number of peripheral methyl groups is increased. Thus, it can be stated that *it is a general property of methylated PAHs to produce a spectral feature in the* 2750–2720 cm^{-1} (3.64–3.68 μm) *region.*

The molecular vibration responsible for this band has not been discussed in any detail in the literature. A careful examination of the spectra reveals that the weak 2740 cm^{-1} (3.65 μm) band is always accompanied by a band in the vicinity of 1380 cm^{-1} (7.25 μm) that is typically about 10 times stronger. This suggests that the 2740 cm^{-1} (3.65 μm) is the first overtone of the vibration causing the 1380 cm^{-1} (7.25 μm) feature. The correlation of the appearance of the 2740 and 1380 cm^{-1} bands with methyl groups suggests that the features are associated with the symmetric deformation vibration of the methyl group on the aromatic ring to which it is attached. The symmetric deformation mode is normally much weaker than the asymmetric deformation mode near 1480 cm^{-1} (6.76 μm) because it produces a smaller dipole oscillation. The presence of the adjacent aromatic ring seems to alter the dipole moment change associated with the symmetric deformation mode, thereby increasing its infrared band strength. The assignment of the 2740 and 1380 cm^{-1} bands to the symmetric deformation mode in methyl sidegroups is supported by the observation that these bands are weaker or absent when the methyl groups are replaced by larger aliphatic sidegroups. Apparently the influence of the aromatic ring on the symmetric methyl deformation mode is greatly reduced when one or more $-CH_2-$ groups intervene. For the reasons stated above, I therefore identify the 1380 and 2740 cm^{-1} bands with the fundamental and first overtone deformation vibrations of $-CH_3$ groups on PAHs. This assignment is consistent with the suggestion by Fuson & Josien (1956) that the 2735 cm^{-1} band of methylated benzanthracenes might be associated with the first overtone of a symmetric $-CH_3$ deformation vibration.

The absolute strength of this feature is not well determined for most PAHs. In their work. Fuson & Josien (1956) report 3055, 2945, and 2735 cm^{-1} band intensities for the monomethyl derivatives of methylbenzene (toluene) and methylnaphthalene and all of the monomethyl, as well as several of the dimethyl, derivatives of benzo[a]anthracene. Averaging over all of the peripheral sites they investigate, and accounting for the different numbers of bonds involved in each case. I find an average of 1.03 $\pm$ 0.44 for the 2735 cm^{-1} (per methyl group) to 3055 cm^{-1} (per aromatic C–H bond) intensity ratio and an average of 0.86 $\pm$ 0.38 for the corresponding 2735 cm^{-1} (per methyl group) to 2945 cm^{-1} (per aliphatic C–H bond) intensity ratio. Examination of the relative strengths of these same bands in the spectra of other PAHs (see Table 2) suggests that these values are probably typical of methylated PAHs in general.

Armed with the information presented above, it is possible to use the nondetection of a band in the spectrum shown in Figure 2 to place an upper limit on the abundance of methyl sidegroups on the PAHs in NGC 7027. The baseline shown in Figure 2 was derived by fitting a second-order polynomial to the data set after the atomic and molecular hydrogen lines were removed. When this baseline and the emission line contributions are removed, the residual flux in the 2790–2690 cm^{-1} (3.58–3.72 μm) range is very small (Fig. 4). Since the 2740 cm^{-1} (3.65 μm) $-CH_3$ feature has a FWHM of 20–40 cm^{-1}, it should cover six to 12 detectors in the high-resolution spectrum of NGC 7027. Comparing the sum of the fluxes in all the detectors in Figure 4 with the sum of the flux in the 2740 cm^{-1} (3.65 μm) region binned in groups of six, nine, and 12 detectors, I derive a conservative upper limit to the integrated strength of the $-CH_3$ feature of $\sim 4 \times 10^{-17}$ W m^{-2}. The average intensities of the 3040 and 2940 cm^{-1} (3.29 and 3.40 μm) features reported for NGC 7027, when scaled to the CGAS aperture

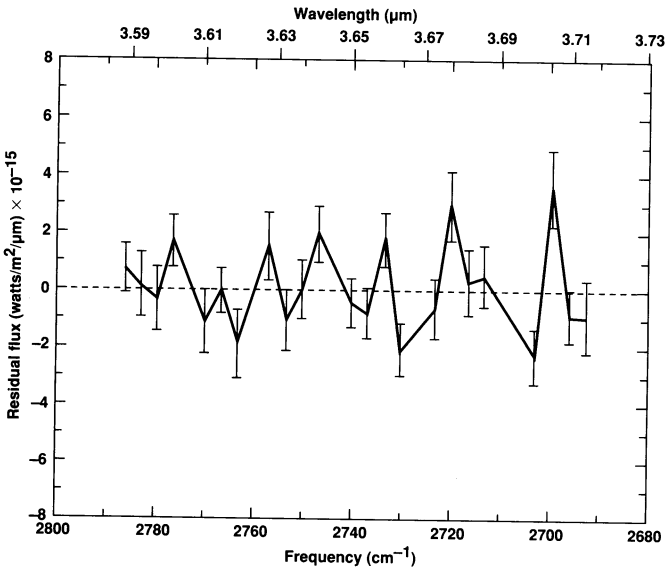

FIG. 4.—The residual flux observed from NGC 7027 after the baseline and emission-line contributions shown in Fig. 2 are removed.

size of 2".7, are about 1.6×10^{-14} W m^{-2} and 1.5×10^{-15} W m^{-2}, respectively (Geballe et al. 1985; Nagata et al. 1988; this work). These values correspond to an upper limit of ~ 0.0025 for the 2740 cm^{-1} (3.65 μm, $-CH_3$ deformation) to 3040 cm^{-1} (3.29 μm, aromatic C–H stretch) intensity ratio and an upper limit of ~ 0.027 for the 2740 cm^{-1} (3.65 μm, $-CH_3$ deformation) to 2940 cm^{-1} (3.40 μm, aliphatic C–H stretch) intensity ratio. Scaling these values by the relative absolute strengths of these three bands discussed in the previous paragraph. I find the following constraints for PAHs in NGC 7027: *(1) the upper limit of the* 2740 cm^{-1} *to* 3040 cm^{-1} *ratio implies that there are* ***at least*** 400 *aromatic* C–H *bonds for every peripheral methyl group, and (2) the upper limit of the* 2740 cm^{-1} *to* 2940 cm^{-1} *ratio implies that there are* ***at least*** 30 *aliphatic* C–H *bonds for every peripheral methyl group.*

The first constraint provides an upper limit to the abundance of $-CH_3$ groups on the PAHs in NGC 7027 that is a factor of *at least* 2–12 times lower than their expected abundances derived in the previous section using the relative strengths of the 2940, 2890, and 2850 cm^{-1} (3.40, 3.46, and 3.51 μm) features. This, of course, is a serious inconsistency with the sidegroup model. An additional fundamental flaw is apparent from the second constraint. If NGC 7027 contains 30 aliphatic C–H bonds for every peripheral methyl group, and if all the aliphatic C–H bonds are in methyl groups, we are lead to the obviously fallacious conclusion that there are ~ 10 methyl groups per methyl group in NGC 7027! This discrepancy could be resolved if we assume that the sidegroups on the PAHs are larger. For example, a 30 to 1 ratio of aliphatic C–H bonds to methyl groups could be accommodated if the PAHs in NCG 7027 carry 5–6 ethyl ($-CH_2CH_3$) groups for every methyl group *and* if we assume the ethyl groups contribute no emission at 2740 cm^{-1} (3.65 μm) (which is not strictly true). However, such a preponderance of larger aliphatic groups is in direct contradiction to the constraints determined in the previous section from the relative strengths of the 2940, 2890, and 2850 cm^{-1} (3.40, 3.46, and 3.51 μm) features.

This and the previous sections can thus be summarized as follows: (1) comparison of the strengths of the 3040, 2940, 2890, and 2850 cm^{-1} (3.29, 3.40, 3.46, and 3.51 μm) features in the spectrum of NGC 7027, in conjunction with the assumption that the latter three bands are due to aliphatic sidegroups on PAHs, leads to several serious inconsistencies in the inferred abundances of the sidegroups; (2) these inconsistencies are smallest (but still present) if the sidegroup population is assumed to be dominated by methyl ($-CH_3$) groups, and (3) the absence of an emission feature near 2740 cm^{-1} (3.65 μm) in the spectrum of NGC 7027 places an upper limit on the abundance of methyl groups on the PAHs in this object which is in direct contradiction to items (1) and (2).

Thus, the large number of inconsistencies inherent in the sidegroup model imply that the 2940, 2890, and 2850 cm^{-1} (3.40, 3.46, and 3.51 μm) features are *not* largely due to aliphatic sidegroups on PAHs. It may still be argued, as is done by Jourdain de Muizon et al. (1990), that the inconsistencies pointed out above might be resolved by invoking sidegroups on ionized, dehydrogenated, or electronically highly excited PAHs. However, such perturbations would have to simultaneously alter four band positions and all their relative intensities in a very specific way while simultaneously leaving the fundamentals of the aromatics largely unchanged. Such an occurrence seems extremely unlikely, and evidence for it will have to be obtained experimentally before it can be seriously considered. In this respect, the burden of proof lies squarely on the proponents of the sidegroup theory.

Finally, it is worth pointing out that this work does not speak directly to the anharmonicity model. However, in light of the many problems associated with the sidegroup model, anharmonicity of the C–H stretch and overtones of the various C–C skeletal vibrations of the PAHs would presently appear to be the leading contenders for the main source(s) of the 2940, 2890, and 2850 cm^{-1} (3.40, 3.46, and 3.51 μm) features. It is important to note that if PAHs are present in the interstellar medium, then bands due to their anharmonic and overtone vibrations *have* to be present in their spectra at some level, *independent of whether they have sidegroups or not.*

4. CONCLUSIONS

The 2790–2690 cm^{-1} (3.58–3.72 μm) infrared emission spectrum of NGC 7027 contains 4 narrow emission lines. Three of the lines fall near 2773, 2743, and 2710 cm^{-1} (3.606, 3.645, and 3.690 μm) and are identified with the $(20 \rightarrow 6)$, $(19 \rightarrow 6)$, and $(18 \rightarrow 6)$ Humphreys series transitions of atomic hydrogen, respectively. The strengths of these lines are consistent with those expected from the observed intensity of the Pfund-γ $(8 \rightarrow 5)$ line in this object. The fourth line falls near 2760 cm^{-1} (3.623 μm) and is identified here with the $(0 \rightarrow 0)$ $S(15)$ transition of molecular hydrogen. The $(0 \rightarrow 0)$ $S(15)$ H_2 line seems to be quite bright and it is not presently clear whether its strength relative to the previously detected H_2 lines in this object is consistent with emission pumped by shocks or ultraviolet photons. Potentially we are seeing evidence of an inverted energy population. In any event, the strength of this band may ultimately provide useful constraints on the molecular H_2 environment in NGC 7027, but it is clear that additional observations of the various H_2 lines must be made using the same aperture and beam positions.

It was found that the relative strengths of the 2940, 2890, and 2850 cm^{-1} (3.40, 3.46, and 3.51 μm) emission features in the spectra of NGC 7027 are inconsistent with the suggestion that they are primarily due to the presence of aliphatic sidegroups on PAHs. The discrepancies between the observed strengths of

the bands and those predicted by the aliphatic sidegroup model are minimized (but not eliminated) if the sidegroups are assumed to consist predominantly of methyl ($-CH_3$) groups. However, if sufficient methyl groups are present to explain the strength of the 2940 cm^{-1} (3.40 μm) feature, then the 2740 cm^{-1} (3.65 μm) overtone of the symmetric methyl deformation mode should also be apparent in the spectrum of NGC 7027. The non-detection of this feature places a severe upper limit on the number of methyl sidegroups present in this object. The PAH population in NGC 7027 must contain *at least* 400 peripheral aromatic C–H bonds for every peripheral methyl group. This $-CH_3$ abundance is a factor of 2–12 times too low to explain the strengths of the 2940, 2890, and 2850 cm^{-1} (3.40, 3.46, and 3.51 μm) features. These various inconsistencies strongly indicate that the 2940, 2890, and 2850 cm^{-1} (3.40, 3.46, and 3.51 μm) interstellar emission features are *not* predominantly due to aliphatic sidegroups on PAHs.

Thus, while aliphatic sidegroups may exist on interstellar PAHs, their abundance must be small, and they do not contribute appreciably to the emission features in the 3300–2800 cm^{-1} (3.0–3.6 μm) region. At present, the best candidates for the source(s) of the 2940, 2890, and 2850 cm^{-1} (3.40, 3.46, and 3.51 μm) emission features are anharmonicity of the aromatic C–H stretching vibration and/or overtones and combination bands of lower frequency PAH vibrations.

The author would like to thank L. Allamandola, F. Salama, and K. Sellgren for assistance in obtaining the data at the IRTF. In addition, L. Allamandola helped with many useful discussions about the properties of PAHs. The author also owes a depth of gratitude to M. Burton, T. Geballe, D. Hollenbach, A. G. G. M. Tielens, and D. Wooden for their assistance in the interpretation of the atomic and molecular hydrogen lines. This paper benefited from a thoughtful review by an anonymous referee. This work was supported by NASA grant 188-44-57-01-00.

REFERENCES

Allamandola, L. J., Tielens, A. G. G. M., & Barker, J. R. 1985, ApJ, 290, L25
———. 1989, ApJS, 71, 733
Barker, J. R., Allamandola, L. J., & Tielens, A. G. G. M. 1987, ApJ, 315, L61
Bellamy, L. J. 1960, The Infra-red Spectra of Complex Molecules (New York: John Wiley and Sons)
Bishop, D. M., & Cheung, M. L. 1982, J. Phys. Chem. Ref. Data, 11, 119
Bregman, J. D., Dinerstein, H. L., Goebel, J. H., Lester, D. F., Witteborn, F. C., & Rank, D. M. 1983, ApJ, 274, 666
Burton, M., Brand, P., Moorhouse, A., & Geballe, T. 1989, in Infrared Spectroscopy in Astronomy, ed. B. H. Kaldeich (ESA-290) (Paris: ESA), 281
Burton, M. G., Hollenbach, D. J., & Tielens, A. G. G. M. 1990, ApJ, 365, 620
Cyvin, S. J., Cyvin, B. N., Brunvoll, J., Whitmer, J. C., & Klaeboe, P. 1982, Zs. Naturforsch, 37a, 1359
Duley, W. W., & Williams, D. A. 1981, MNRAS, 196, 269
Ellis, H. B., & Werner, M. W. 1984, BAAS, 16, 462
Fox, J. J., & Martin, A. E. 1939, J. Chem. Soc., p. 318
Fuson, N., & Josien, M. L. 1956, J. Am. Chem. Soc., 78, 3049
Geballe, T. R. 1983, in Proc. of the Workshop on Laboratory and Observational Spectra and Interstellar Dust, ed. R. D. Wolstencroft & J. M. Greenberg (Occasional Reports of the Royal Observatory: Edinburgh), 93
Geballe, T. R., Lacy, J. H., Persson, S. E., McGregor, P. J., & Soifer, B. T. 1985, ApJ, 292, 500
Geballe, T. R., Tielens, A. G. G. M., Allamandola, L. J., Moorhouse, A., & Brand, P. W. J. L. 1989, ApJ, 341, 278
Gribov, L. A., & Smirnov, V. N. 1962, Soviet Phys.—Uspekhi, 4, 919
Hummer, D. G., & Storey, P. J. 1987, MNRAS, 224, 801
Jourdain de Muizon, M., d'Hendecourt, L. B., & Geballe, T. R. 1990, A&A, 235, 367
Jourdain de Muizon, M., Geballe, T. R., d'Hendecourt, L. B., & Baas, F. 1986, ApJ, 306, L105
Masson, C. R., et al. 1985, ApJ, 292, 464
Merrill, K. M., Soifer, B. T., & Russell, R. W. 1975, ApJ, 200, L37
Nagata, T., Tokunaga, A. T., Sellgren, K., Smith, R. G., Onaka, T., Nakada, Y., & Sakata, A. 1988, ApJ, 326, 157
Reddy, K. V., Heller, D. F., & Berry, M. J. 1982, J. Chem. Phys., 76, 2814
Russel, R. W., Soifer, B. T., & Merrill, K. M. 1977a, ApJ, 213, 66
Russell, R. W., Soifer, B. T., & Willner, S. P. 1977b, ApJ, 217, L149
Sandford, S. A., Allamandola, L. J., Tielens, A. G. G. M., Sellgren, K., Tapia, M., & Pendleton, Y. 1991, ApJ, 371, 607
Seaton, M. J. 1979, MNRAS, 187, 785
Smith, H. A., Larson, H. P., & Fink, U. 1981, ApJ, 244, 835
Swofford, R. L., Long, M. E., & Albrecht, A. C. 1976, J. Chem. Phys., 65, 179
Tokunaga, A. T. 1986, IRTF Photometry Manual, University of Hawaii
Tokunaga, A. T., Smith, R. G., & Irwin, E. 1987, in Infrared Astronomy with Arrays, ed. C. G. Wynn-Williams, E. E. Becklin, & L. H. Good (Honolulu: Univ. of Hawaii), 367
Treffers, R. R., Fink, U., Larson, H. P., & Gautier, T. N., III. 1976, ApJ, 209, 793
Wexler, A. S. 1967, Appl. Spectrosc. Rev., 1, 9
Wiese, W. L., Smith, M. W., & Glennon, B. M. 1966, Atomic Transition Probabilities, Vol. 1—Hydrogen through Neon (NSRDS-NBS4) (Washington, DC: NBS)
Witteborn, F. C., Sandford, S. A., Bregman, J. D., Allamandola, L. J., Cohen, M., Wooden, D. H., & Graps, A. L. 1989, ApJ, 341, 270